Quaternary Science Reviews 157 (2017) 129–140

Contents lists available at ScienceDirect

Quaternary Science Reviews

journal homepage: www.elsevier.com/locate/quascirev

Climate variability in the past ~19,000 yr in NE Tibetan Plateau inferred from biomarker and stable isotope records of Lake Donggi Cona

Jeetendra Saini [a], Franziska Günther [a], Bernhard Aichner [b], Steffen Mischke [c], Ulrike Herzschuh [b], Chengjun Zhang [d], Roland Mäusbacher [e], Gerd Gleixner [a, *]

[a] Max Planck Institute for Biogeochemistry, 07745 Jena, Germany
[b] Institute for Earth and Environmental Sciences, University of Potsdam, 14476 Potsdam, Germany
[c] School of Engineering and Natural Sciences, University of Iceland, Iceland
[d] College of Geological Sciences and Mineral Resources, Lanzhou University, Lanzhou, China
[e] Friedrich Schiller University, Institute for Geography, 07747 Jena, Germany

ARTICLE INFO

Article history:
Received 13 April 2016
Received in revised form
13 October 2016
Accepted 27 December 2016
Available online 2 January 2017

Keywords:
n-alkanes
Hydrogen isotopes (δD)
Carbon isotopes ($\delta^{13}C$)
Carbon preference index (CPI)
Westerlies
Continental air masses
Precipitation
Late Glacial and Holocene

ABSTRACT

We investigated 4.84-m-long sediment record spanning over the Late Glacial and Holocene from Lake Donggi Cona to be able to reconstruct circulation pattern on the Tibetan Plateau (TP). Presently, Lake Donggi Cona is located at the boundaries of Westerlies and Asian monsoon circulations in the north-eastern TP. However, the exact timing and stimulating mechanisms for climatic changes and monsoon shifts in this region are still debated. We used a 19-ka-long stable isotope record of sedimentary *n*-alkanes to address this discrepancy by providing insights into paleohydrological conditions. The δD of nC_{23} is influenced by lake water evaporation; the δD values of sedimentary nC_{29} are mainly controlled by moisture source and temperature changes.

Long-chain *n*-alkanes dominate over the core whereas three mean clusters (i.e. microbial, aquatic and terrestrial) can be inferred. Multi-proxies suggest five major episodes in the history of Lake Donggi Cona. The Lake Donggi Cona record indicates that the Late Glacial (18.4–14.8 cal ka BP) was dominated by low productivity of mainly microbial and aquatic organisms. Relatively low δD values suggest low temperatures and moist conditions eventually caused by stronger Westerlies, winter monsoon and melt-water influence. Likely, the shift (~17.9 cal ka BP) from microbial to enhanced aquatic input suggests either a change from deep to shallow water lake or a break in local stratification. Between 14.8 and 13.0 cal ka BP, variable climatic conditions prevailed. Although the Westerlies weekend, the increase in temperature enhanced the permafrost and snow melting (displayed by a high sedimentary accumulation rate). Higher δD values indicate increasingly arid conditions with higher temperatures which eventually lead to high evaporative conditions and lowest lake levels. Low vegetation cover and high erosion rates led to high sediment accumulation resulting in stratification followed by anoxia in the terminal lake. From 13.0 to 9.2 cal ka BP, lowered values of δD along with high contents of terrestrial organic matter marked the early-Holocene warming indicating a further strengthening of summer precipitation and higher lake levels. A cooling trend was observed in the mid-Holocene between 9.2 and 3.0 cal ka BP accompanied by higher moisture availability (displayed by lowered δD values) caused by reduced evaporative conditions due to a drop in temperature and recovering Westerlies. After 3.0 cal ka BP, a decrease in lake productivity and cold and semi-arid conditions prevailed suggesting lower lake levels and reduced moisture from recycled air masses and Westerlies. We propose that the summer monsoon was the predominant moisture source during the Bølling-Allerød warm complex and early-Holocene followed by Westerlies in mid-to-late Holocene period. Stable carbon isotope values ~ - 32‰ indicate the absence of C_4-type vegetation in the region contradicting with their presence in the Lake Qinghai record. The δD record from lake Donggi Cona highlights the importance of the interplay between Westerlies and summer monsoon circulation at this location, which is highly dynamic in northeastern plateau compared to the North

* Corresponding author.
E-mail address: gerd.gleixner@bgc-jena.mpg.de (G. Gleixner).

http://dx.doi.org/10.1016/j.quascirev.2016.12.023

Atlantic circulation and insolation changes. Consequently lake Donggi Cona might be an important anchor point for environmental reconstructions on the Tibetan Plateau.

1. Introduction

Lake level fluctuations and moisture evolution at the Tibetan Plateau (TP) are closely related with large scale environmental changes. The TP is one of the most extensive and sensitive regions of elevated topography affecting regional and global climate. However, its high-altitude topography (>4000 m above sea level) also makes it sensitive to direct insolation heating and atmospheric circulation changes. Due to the elevated topography of the TP, it hinders the Westerlies and splits them into northward and southward branches likewise Himalaya splits the Asian monsoon into northward and eastward branches. The spatio–temporal extent of monsoonal circulating on in the region is still uncertain especially in the northeastern plateau. Lake Qinghai, located ca. 230 km northeast of Lake Donggi Cona, has been reported to be influenced by both mid-latitude Westerlies and Asian summer monsoon (Liu et al., 2015). They proposed the dominating influence of Westerlies over the Last Glacial Maximum (LGM) until 11.5 cal ka BP and an abrupt strengthening of the Asian monsoon in the Holocene (An et al., 2012b). The quest to understand past climatic changes and the interplay between the Asian monsoon and the Westerlies has been the focus for the last few decades, especially in the northern part of the TP (An et al., 2012a; Chen et al., 2008; Mischke et al., 2008; Morrill et al., 2003; Shen et al., 2005a, b; Wang et al., 2005; Zhao et al., 2007). However, it is still ambiguous whether the general climate history at the TP since the LGM is similar to those of areas influenced by Asian summer monsoon (An, 2000; Herzschuh et al., 2009; Morrill et al., 2003). The climate history differs between areas of different precipitation/evaporation (P/E) ratios i.e. the early Holocene was apparently drier in areas of low P/E ratios such as the Bayanbulak Basin, NW China, in comparison to areas of high P/E ratios such as the southern TP (Herzschuh et al., 2009; Long et al., 2014). The influence of different atmospheric circulation systems are of critical importance for the moisture and climate evolution in the region. The snow cover and albedo effect are also considered to have large-scale effects on the atmospheric circulation (Kang et al., 2010; Ma et al., 2009; Wu and Qian, 2003). The glaciers at the TP are currently experiencing significant melting due to anthropogenic climate warming (Qin and Xiao, 2009; Tian et al., 2006; Yao et al., 1996, 2013).

Most studies of the last few decades dealt with proxy records from lake sediments displaying hydrological and related sedimentary processes to infer climatic and environmental changes (Chen et al., 2001, 2006, Chen and Holmes, 2003; Herzschuh et al., 2004, 2006b; Ji et al., 2005; Mügler et al., 2010; Shen et al., 2005b). A key approach is the reconstruction of moisture availability, which evolved regionally asynchronous throughout the Holocene and Late Pleistocene (An et al., 2000; Chen et al., 2008; Hartmann and Wünnemann, 2009; Herzschuh et al., 2006b). Furthermore, it is still unclear whether the precipitation or temperature changes have been dominant features of the observed environmental changes, especially in the northeastern TP. The hydrological variations of lake Donggi Cona are not only controlled by precipitation through local and regional sources, inflow/outflow ratio, surface air temperature but are also affected by surface runoff, underground recharge, glacial melt-water and lake water evaporation. The lake catchment has been partially influenced by glacial melt-water inflow at least during the LGM and the early to late Glacial period (IJmker et al., 2012a, b).

Lake Donggi Cona is very sensitive to climatic variations and thus has been the focus for several studies covering the Late Glacial and Holocene period. Detailed studies include sedimentation rate of lacustrine sediments (Opitz et al., 2012), basin morphology and related sedimentary processes (Dietze et al., 2010), ostracods, carbonate content, pollen spectra and other bulk sedimentological proxies (Aichner et al., 2012; Opitz et al., 2012; Wang et al., 2014). However these investigations mainly focused on bulk organic matter or single proxies.

In this paper, we present sedimentary *n*-alkanes and compound-specific hydrogen and carbon isotopes to investigate the source of organic matter as well as moisture and temperature variability over the past 19,000 yr and gain further insights into the monsoonal and climatic history of lake Donggi Cona in the semi-arid northeastern TP. Additionally, we compare our results with existing paleo-records from the Tibetan Plateau to improve our understanding of the regional paleoclimatic changes.

2. Study site

Lake Donggi Cona, also known as Dongxi Co, is located in the northeastern part of the TP (35°18′N, 98°32′E, 4090 m a.s.l.) in the Qinghai province of China (Fig. 1A). It is located in the southeast of A'nyemaqen and in the west of Kunlun mountain ranges that are presently deglaciated (Dietze et al., 2010). The left lateral Kunlun Fault intersects the Lake Donggi Cona catchment from WNW to ESE. Lake Donggi Cona fills the western half of 60 km long to 20 km wide pull apart basin, with a catchment area of 3174 km^2. The lake has the dimension of approximately 31 km by 8 km and a surface area of 229 km^2. The maximum water depth reaches up to 98 m (Mischke et al., 2010a). The lake catchment consists of clastic rocks dating back to Permian to Neogene limestone and granite and sandstone of middle Triassic age (Dietze et al., 2010). The lake has mainly two perennial inflows from the east and northeast and some seasonal inflows from north and south. The presence of U-shaped valleys with lateral moraines and V-shaped valleys are found on the northwestern side of lake catchment, indicating former glacial activity and fluvial transport in the past (IJmker et al., 2012a, b; Opitz et al., 2012). The outflow of the lake is gauged by artificial station since 1970s that feeds a river and eventually enters into Qaidam Basin in the northwestern TP. The mean annual surface air temperature is −4.1 °C (Madoi Climate station, Chinese Central Meteorological Office, 2008). Most of the rainfall (~85%) occurs during the summer season from June to October with 304 mm of annual precipitation. The δD values in precipitation water from Madoi weather station (50 km southwest of Donggi Cona) (Fig. 2) indicate a strong correlation between δD of precipitation and surface air temperature ($r^2 = 0.52$, $p < 0.03$) and a weak correlation, for δD and precipitation amount ($r^2 = 0.22$, $p < 0.03$) based on event based rain and snow fall measurements (Ren et al., 2013). This demonstrates that surface air temperature plays the most important and influencing role on precipitation which overprints the effect of the precipitation amount. However, over long term moisture source affect the variation in δD record. Vegetation in this semi-arid region primarily consists of alpine meadows in the

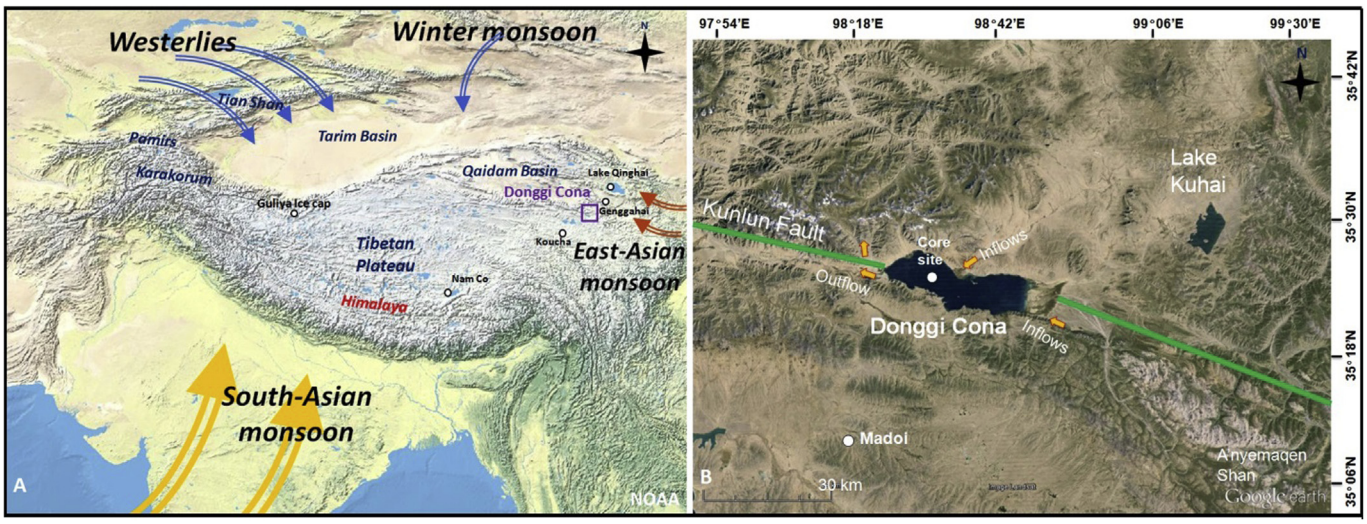

Fig. 1. (A) Different atmospheric circulations at the Tibetan Plateau, Lake Donggi Cona (purple square), Guliya ice cap and other nearby lakes mentioned in the text such as Genggahai (Rao et al., 2014), Koucha (Herzschuh et al., 2009), Nam Co (Mügler et al., 2010; Günther et al., 2015) and Qinghai (Shen et al., 2005a,b; An et al., 2012b). (B) Topographic map of Lake Donggi Cona with core site PG1790, Kunlun fault (green lines) and Madoi weather station (50 km south west of Donggi Cona). (For interpretation of the references to colour in this figure legend, the reader is referred to the web version of this article.)

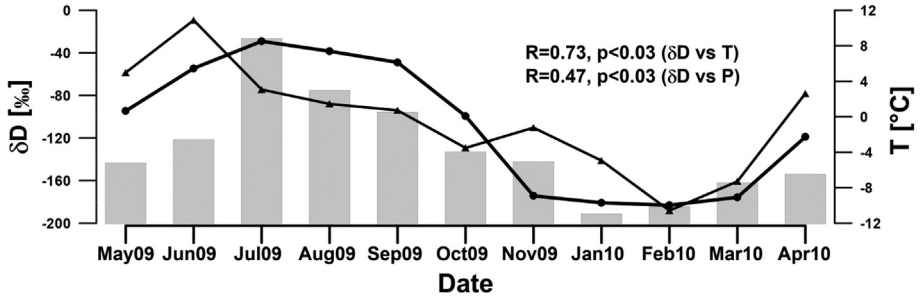

Fig. 2. Temporal variations of δD in precipitation (dots), surface air temperature (triangle) and precipitation amount (bar) from May 2009–April 2010 at Madoi meteorological station, China (Ren et al., 2013).

uplands dominated by *Kobresia*, alpine steppes on the vast plains composed mainly of Poaceae and *Artemisia* (Kürschner et al., 2005). The mountains in the direct vicinity of Lake Donggi are covered by mountain shrub lands.

3. Materials and methods

3.1. Coring and chronology

The sediment core PG1790 was collected in February 2007 in the eastern part of Lake Donggi Cona (35.345°N, 98.436°E) from ice-cover with an UWITEC piston corer 'Niederreiter 60' and an UWITEC corer for short cores. The water depth at the core site was 34.7 m. The four core segments with a composite length of 4.84 m were obtained with a mean overlap of 20 cm. The age-model for the core is based on ^{14}C-AMS dating results of total organic carbon (TOC) (Mischke et al., 2010a). The topmost 1 cm, surface sample along with 'humic' and 'humin' fraction of samples were used to calculate the reservoir effect that is 1983 ± 30 years for TOC. The ^{14}C age of the topmost sample is subtracted from other samples to get the correct ages assuming that the reservoir effect was constant through time. Based on the already published chronology (Aichner et al., 2012; Mischke et al., 2010a; Opitz et al., 2012), the sediment core covers the past ~18.6 cal ka BP with an average sedimentation rate of 25.5 cm/ka. Based on the published chronology and our results we can see five periods based on the sediment accumulation rates (SAR): between 18.4 and 14.8 cal ka BP the SAR is 25 cm/ka, between 14.8 and 13.0 cal ka BP SAR shows significantly high values of 95 cm/ka, between 13.0 and 9.2 cal ka BP it is 18 cm/ka, between 9.2 and 3.0 cal ka BP it is 14 cm/ka and between 3.0 and 1.2 cal ka BP it is 20 cm/ka (Fig. 4).

3.2. Sample preparation, n-alkane extraction and quantification

85 samples were processed for *n*-alkane analysis after freeze drying and grinding prior to extraction. The extraction was performed with a 9:1 mixture of dichloromethane/methanol at 100 °C and 2000 psi for 15 min in 2 cycles using an accelerated solvent extractor (ASE200, Dionex Corp., Sunnyvale, USA). Total dry weight of samples varied from 2.8 to 10 g depending upon total organic carbon content. The aliphatic hydrocarbon fractions were separated from other components using silica gel column chromatography with hexane as solvent for the *n*-alkane fraction. The qualitative and quantitative analysis of *n*-alkanes was performed on gas chromatography coupled with flame ionization detector (GC-FID; Agilent Technology HP6890 Series GC system). Injector is heated from 60 °C to 330 °C operating in splitless mode with DB-1ms silica capillary column (50 m, 0.32 mm inner diameter, 0.52 μm film thickness). Helium carrier gas flow was kept constant at 2.0 ml min^{-1} The oven was maintained for 1 min at 60 °C, heated at

5 °C/min to 320 °C (maintained for 10 min) and finally heated at 30 °C min^{-1} to 330 °C (maintained for 3 min). To visualize various sources of lacustrine *n*-alkanes, hierarchical K-mean cluster analysis of the sedimentary *n*-alkanes was performed using SPSS 17.0 software based on the relative abundance of *n*-alkanes (Gao et al., 2011). Additionally, the *n*-alkane carbon preference index (CPI) (Bray and Evans, 1961), average chain length (ACL) (Poynter and Eglinton, 1990), aquatic to terrestrial ratio (P_{aq}) (Ficken et al., 2000) and the offset between nC_{23} and nC_{29} ($\Delta\delta D_{C23\text{-}C29}$) (Mügler et al., 2008) was calculated using following equations:

$$CPI_{16-33} = \frac{1}{2} * \left[\left(\sum C_{17-33}\right)\Big/\left(\sum C_{16-30}\right) + \left(\sum C_{17-33}\right)\Big/ \times \left(\sum C_{18-32}\right)\right] \quad (1)$$

$$ACL_{16-33} = \left(\sum C_n * n\right)\Big/\left(\sum C_n\right) \quad (2)$$

$$P_{aq} = (C_{23} + C_{25})/(C_{27} + C_{29} + C_{31}) \quad (3)$$

$$\Delta\delta D_{C23-C29} = (\delta D_{C23} - \delta D_{C29}) \quad (4)$$

3.3. Biomarker isotope analysis

The measurements of compound-specific δD values were performed by injecting 1 μl into a coupled GC-IRMS system (GC: HP-7890, Agilent Technology, Palo Alto USA; IRMS: Delta V^{Plus}, Thermo Fisher Scientific, Bremen Germany) equipped with a DB-1ms (30 m, 0.25 mm inner diameter, 0.25 μm film thickness, Agilent). The injector was operated in splitless mode at 280 °C. The oven was maintained for 2 min at 60 °C, heated at 6 °C/min to 320 °C (maintained for 10 min). The carrier gas flow was constant at 1.7 ml min^{-1}. Each sample was measured in triplet with a standard mixture (nC_{15} to nC_{33}) measurement after 3 samples (overall 9 GC injections). The δD values of *n*-alkanes in the standard mixture were calibrated against the international reference substances (NBS-22, IAEA-OH22) using offline TC/EA technique (Gehre et al., 2004). Drift correction was applied and the precision of measurements were expressed as mean standard deviation for all standard mixture in triplicates was 1.4‰. The H_3^+ factor, testing the stable ion source conditions was determined once a day with a constant value of 3.1 (SD = 0.03). For $\delta^{13}C$ measurements we used a coupled GC-IRMS system (GC: HP5890 Agilent Technology, Palo Alto USA; IRMS: Delta XP, Thermo Fisher Scientific, Bremen Germany) equipped with a HP Ultra2 (50 m, 0.32 mm inner diameter, 0.52 μm film thickness, Agilent). The sample measurements follow the same procedure as above while monitoring the standard mixture (SD = 0.28) for machine stability over whole period. The measured isotopic ratios were reported in conventional δD and $\delta^{13}C$ notation relative to V-SMOW and V-PDB standards for hydrogen and carbon, respectively.

$$\delta = \left[\left(R_{sample} - R_{standard}\right)\Big/R_{standard}\right] \times 1000$$

Where R is the $^2H/^1H$ or $^{13}C/^{12}C$ ratio of the samples/standard respectively and the unit is per mil (‰).

Since many of the samples only contained low concentrations of *n*-alkanes, the sample volume was reduced to 20 μl for δD measurements and 60 μl for $\delta^{13}C$ measurements. Only peaks with an intensity over 60 mV were considered for evaluation, which is in linearity for our GC-IRMS system based on serial dilution tests (Günther et al., 2013; Witt et al., 2016). ISODAT NT 2.0 workspace package (Thermo Fisher Scientific, Bremen, Germany) was applied for background correction for δD and $\delta^{13}C$ values.

4. Results

4.1. n-Alkane distribution in lake sediments

In general, the concentrations of total *n*-alkanes ($nC_{15\text{-}33}$) range from 0.1 to 5.7 μg/g dry weight (d.w.) (median: 1.4 μg/g d.w.). The sediments can be separated into three groups by hierarchical mean cluster analysis (Fig. 3). Cluster type-1 is dominated by short even chain nC_{18} and nC_{20}, whereas samples in cluster type-2 are mainly dominated by nC_{23} and nC_{25} and sediments in cluster type-3 are mainly dominated by nC_{29} and nC_{31}. Long-chain *n*-alkanes ($nC_{27\text{-}33}$) far exceed the amount of short ($nC_{15\text{-}21}$) and mid chain ($nC_{21\text{-}25}$) alkanes (Fig. 3A). On average long-, mid-, and short-chain *n*-alkanes amount up to 65%, 22% and 13% respectively in the sediments.

Based upon the *n*-alkanes amounts, CPI, ACL and P_{aq} values, the sediment core can be divided into five distinct periods (Fig. 4). Period 1 (18.4–14.8 cal ka BP) is characterized by a dominance of short and mid-chain *n*-alkanes with average concentrations of 0.22 μg/g d.w.. The CPI values are the lowest with an average of 4.4, while P_{aq} ratios are the highest (>2.3). Period 2 (14.8–13.0 cal ka BP) is characterized by variable, but increasing concentrations of mid and long-chain *n*-alkanes with average values of 0.69 μg/g d.w.. The CPI and P_{aq} values are highly variable with average values of 26.6 and 0.46, respectively. Following period 3 (13.0–9.2 cal ka BP) demonstrates high amounts of long-chain *n*-alkanes with an average value of 2.4 μg/g d.w.. The CPI and P_{aq} values are distinctively lower than in period 2 with an average value of 12.0 and 0.43, respectively. The concentrations of total *n*-alkanes steadily increase from the beginning until reaching maximum values at 9.2 cal ka BP (Fig. 4) followed by a sudden drop after 9.2 cal ka BP. Period 4 (9.2–3.0 cal ka BP) is characterized by a decline in the amounts of *n*-alkanes in the beginning followed by increasing trend towards the end of the period. The *n*-alkane amount shows an average value of 2.61 μg/g dw.. However, period 5 (3.0–1.2 cal ka BP) is characterized by a decline in the amounts of *n*-alkanes in the beginning followed by sudden rise ~1.6 cal ka BP and then declining trend towards end of the period. The *n*-alkane amount shows an average value of 3.40 μg/g d.w.. The CPI values are the highest with an average of 53.0, whereas P_{aq} is at the minimum value of 0.14.

4.2. Stable hydrogen and carbon isotopes of n-alkanes

Compound-specific δD values are considered to be a promising proxy to for paleoclimate and moisture conditions (Günther et al., 2013; Huang et al., 2004; Pagani et al., 2006; Sachse et al., 2006). Here we present the δD and $\delta^{13}C$ records for nC_{23} and nC_{29}. The average δD values for nC_{23} and nC_{29} are −140 ± 28‰ and −162 ± 22‰, respectively. Both show large variations up to 140‰ throughout the sediment core (Fig. 4). The δD values of the mid-chain *n*-alkanes indicate a trend of lowering in period 1 and 3, higher values are recorded in period 2 and 5 and relatively stable values in period 4. The δD values of nC_{29} show a trend of depletion in period 1, 4 and 5 and enrichment in period 2 and 3. δD values of nC_{23} and nC_{29} are correlated ($R = 0.69$, $p < 0.001$), especially in period 3 and 4. The $\delta^{13}C$ values of nC_{23} in period 3, 4 and 5 only show slight variations, while they vary between −27‰ and −32‰ in period 1and 2. $\delta^{13}C$ values of nC_{29} exhibit mean values around −32 ± 1.4‰, whereas the $\delta^{13}C$ of nC_{23} show enriched values around −27 ± 3.2‰ over the core. $\delta^{13}C$ values of nC_{23} and nC_{29} are highly correlated especially in period 2 ($R = 0.69$, $p = 0.003$). $\delta^{13}C$ values of nC_{23} and nC_{29} show comparable down core variations

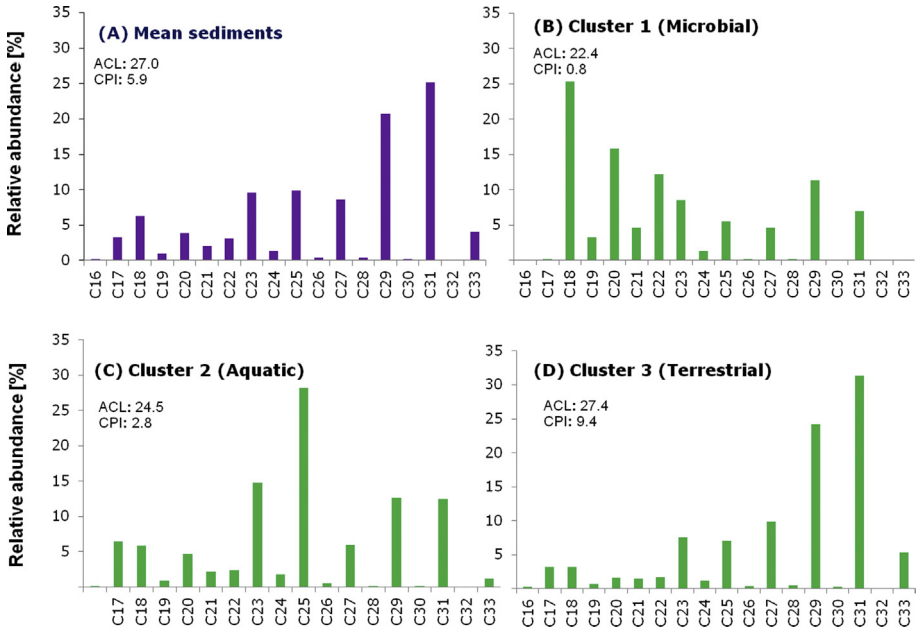

Fig. 3. Relative distribution of total amount of n-alkanes and three principal clusters of n-alkanes over the core.

except in period 2, where $\delta^{13}C$ values of nC_{23} is depleted by ~2‰ compare to other periods. Down core variations in $\delta^{13}C$ values of nC_{29} are less pronounced. We calculated the $\Delta\delta D_{C23\text{-}C29}$ that has been proposed in comparative studies from Nam Co and Lake Hurleg to be indicator of evapotranspiration proxy (Mügler et al., 2008; Rao et al., 2014; Sachse et al., 2006). $\Delta\delta D_{C23\text{-}C29}$ shows positive trend in period 2 and 5 while lower values in period 1, 3 and 4.

5. Discussion

5.1. Source of organic matter

Organic matter in the lacustrine sediments consists of individual molecules that derive from biological sources representing autochthonous and allochthonous input. Their composition and abundances may identify paleo-ecological conditions (Eglinton and Hamilton, 1967; Meyers, 2003). To characterize organic matter in sediments, *n*-alkane proxies have been frequently applied. Relatively high amounts of long-chain *n*-alkanes (high ACL, low P_{aq}) and a high CPI have been interpreted to reflect relative high contributions of fresh and terrestrial organic matter, whereas lower values for CPI and ACL and a higher P_{aq} are characteristic for pronounced aquatic and microbial influences or cyanobacterial source of organic matter, and/or decomposition effects of microorganism activities (Ficken et al., 2000; Pu et al., 2010). For the studied sediment core, the dominant *n*-alkanes are the long chain homologues $nC_{29/31}$ (Fig. 3a). This suggests that the organic matter is primarily derived from terrestrial sources such as terrestrial plants and grass having high amounts of nC_{29} and nC_{31}, respectively (Meyers, 2003). This is supported by relatively stable $\delta^{13}C$ values of those compounds which are in the range of terrestrial C_3-vegetation (Meyers and Ishiwatari, 1993; Meyers and Lallier-Verges, 1999; Oleary, 1988). In a recent survey, Aichner et al. (2010c) estimated the present contribution of aquatic macrophytes to TOC in Lake Donggi Cona to 13% only, based on comparison between highly enriched carbon isotopic values in aquatic plant samples and corresponding surface sediments. The same study inferred that also "aquatic" mid-chain alkanes contain a significant terrestrial proportion of ca. 50–60% and must therefore be considered as derived from mixed sources in this lake. The dominance of terrestrial sources of organic matter has also been deduced from other proxies such as TOC/TN and the presence of higher plant detritus (Aichner et al., 2012). Short and mid-chain *n*-alkanes, however, play a more important role in the oldest section of the core (period 1; ca. 18–15 ka BP), suggesting enhanced proportional aquatic and microbial contribution to TOC and alkanes during this time interval (Fig. 4). This is further supported by relatively high $\delta^{13}C$-values during this episode, which can be explained with the uptake of isotopically enriched bicarbonate by aquatic plants (Allen and Spence, 1981). To conclude, sedimentary organic matter in Lake Donggi Cona is primarily derived from allochthonous/terrestrial sources in period 3, 4, 5 and to a lesser extent in period 2 whereas period 1 is mainly dominated by in-situ aquatic or cyanobacterial source of organic matter.

5.2. Temperature and amount effect on precipitation

At the TP, isotopes in the precipitation can be influenced by several factors. Fundamental studies have revealed the positive relationship between precipitation δD and temperature in the northern TP and Tianshan mountains (Tian et al., 2001; Yao and Thompson, 1992; Yao et al., 2013), whereas strong monsoon activity results in high precipitation rates and highly depleted isotopes in the southern TP. This depletion is attributed to the so called 'amount effect' that results in a poor $\delta^{18}O$ and temperature relationship at both seasonal and annual scales (Tian et al., 2003). In the middle of the Tibetan Plateau, the effects of the monsoon are diminished but continue to cause a reduced correlation between $\delta^{18}O$ and temperature at the annual scale. Competing scenarios such as above, could potentially explain the opposite hydrological changes in the northern/southern regions. For instance, evaporation on the northern Tibetan Plateau might be dominantly affected by temperature changes than precipitation amount compared to the monsoon controlled region. Data from the northern TP indicate strongly enriched values in summer and depleted values in winter, which is comparable to other non-monsoon regions. However, it has to be considered that the TP is a relatively arid region and δD values of the lake water are affected by evaporation and,

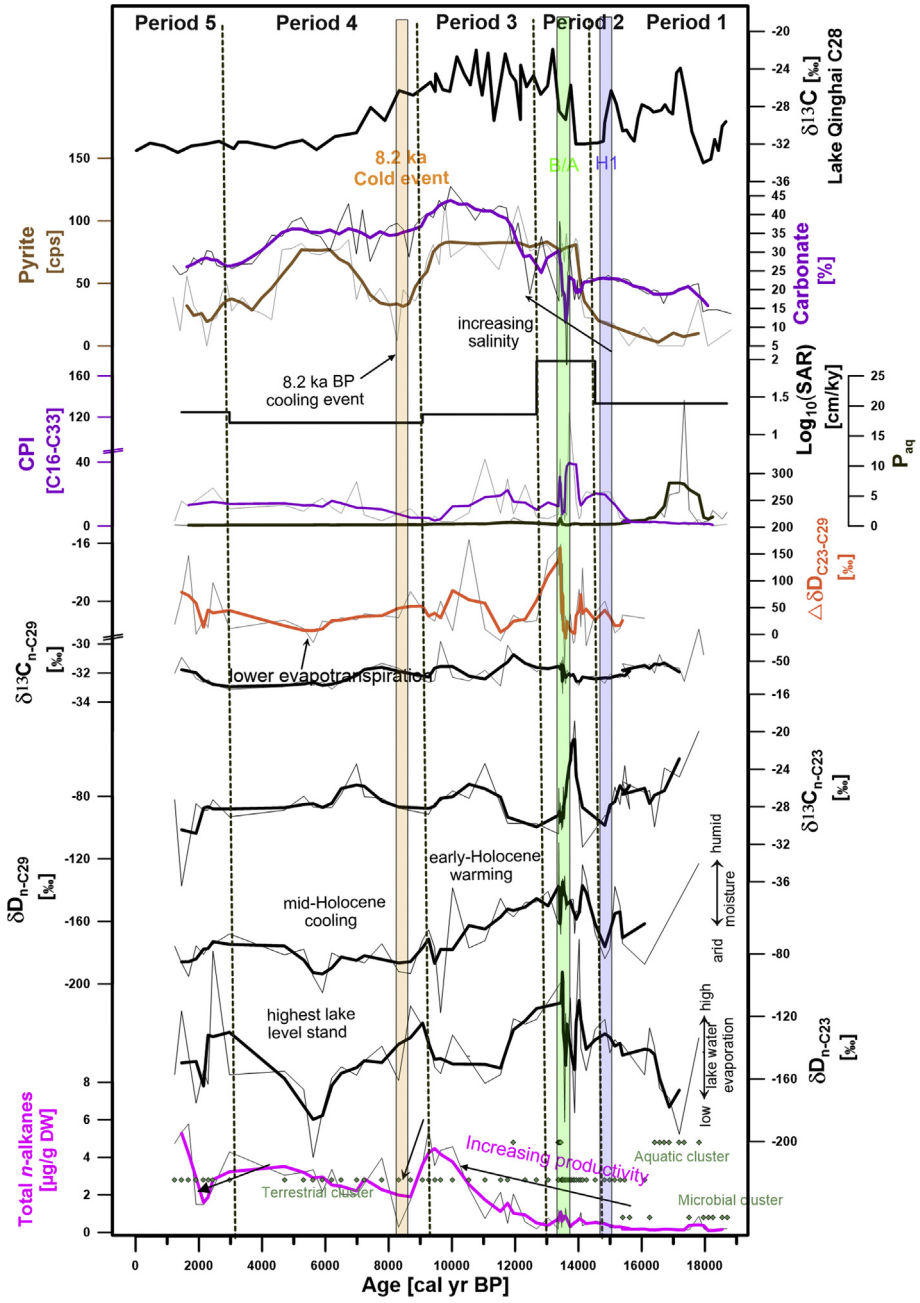

Fig. 4. Multiproxy records of the core PG1790. From bottom to top-total amount of *n*-alkanes with cluster distribution, δD and $\delta^{13}C$ values for nC_{23} and nC_{29}, evapotranspiration proxy $\Delta\delta D_{C23\text{-}C29}$, P_{aq} and CPI distribution over the core, sediment accumulation rate in logarithmic scale (Log_{10} SAR) and pyrite and carbonate distribution over the core (Opitz et al., 2012). The $\delta^{13}C_{wax}$ curve is based on Lake Qinghai core (Thomas et al., 2014). The zonation is based upon the distribution of combined biomarker distribution.

consequently, are even more enriched in deuterium than the original meteoric water (Gat, 1996). Here, the surface air temperature is the controlling factor and overshadows the 'amount effect' of precipitation (Araguas-Araguas et al., 1998). Various mechanisms have been proposed relating monsoon circulation to the precipitation δD i.e. altitude effect, continental effect, upstream distillation of moisture having ambiguous effects on isotopes (Liu et al., 2003). Close to Lake Donggi Cona, at Madoi, a significant effect of surface air temperature on δD values ($R = 0.73$, $p < 0.03$) of precipitation water is recorded. However, the proxy trend with higher δD values during the glacial and subsequent depletion would imply a warmer glacial and cooler Holocene. Hence, temperature can't be the dominant influencing factor on δD of precipitation on longer timescales. Changes in precipitation amount cannot explain the observed variability in δD alone. Thus, we interpret δD values of long-chain *n*-alkanes from Lake Donggi Cona sediments to be driven by changing moisture sources.

5.3. Paleoenvironmental implications of δD and $\delta^{13}C$ record of *n*-alkanes

The growth of terrestrial and aquatic plants are primarily controlled by temperature, salinity and water availability, hence the amount of *n*-alkanes do not only reflect the biological productivity, but also indicate the climatic conditions. Higher amounts of *n*-alkanes can be linked with higher biological productivity associated

with rising temperature and higher summer precipitation. For this study, we particularly focus on the sedimentary *n*-alkanes nC_{23} and nC_{29}, that have been proved to be very useful tools in comparable studies (Günther et al., 2013; Mügler et al., 2008). The δD values of long-chain *n*-alkanes mainly derived from terrestrial sources (e.g. nC_{29}) reflect the isotopic signature of meteoric water modified by evapotranspiration and/or other meteorological factors, whereas the δD values of mid-chain *n*-alkanes which are at least proportionally derived from aquatic sources (e.g. nC_{23}) also record the isotopic composition of the corresponding lake water modified by evaporation (Günther et al., 2013; Pagani et al., 2006). Additionally we used the isotopic difference between nC_{23} and nC_{29} ($\Delta\delta D_{C23\text{-}C29}$) that indicates changes in effective moisture and evapotranspiration (Mügler et al., 2008). The organic geochemical parameters (total *n*-alkanes, *n*-alkane ratios, stable hydrogen and carbon isotope) from our record (Fig. 4) were compared with other proxies from the core (i.e. salinity inferred from specific conductivity based on ostracods) (Mischke et al., 2010a) and pyrite/carbonate content (Opitz et al., 2012). Based on the results of this multiproxy approach the development of Lake Donggi Cona is discussed in the five separated climate periods (Fig. 4).

5.3.1. Late Glacial and Holocene climatic history of Lake Donggi Cona

5.3.1.1. Period 1 (4.8–3.7 m, 18.4–14.8 cal ka BP). The *n*-alkane pattern in the lower part of the core, predominantly of microbial origin in the beginning of the period indicates a deep water lake that favors the microbial growth instead of aquatic plants. After 17.5 cal ka BP, the shift from deep water lake to shallow water lake was probably accompanied by a change from microbial-dominated to macrophyte-dominated lake. The lower CPI (mean 4.41) and higher P_{aq} ratios (0.5) suggest a dominance of submerged macrophytes in the lake. Clearly, the cold conditions are not conducive to the growth of submerged and/or terrestrial plants, ultimately, resulted in the relatively low amounts of *n*-alkanes. The terrestrial plants, however, played a minor role during that episode. The lower δD values of nC_{23} (mean −145‰), nC_{29} (mean −184‰) and $\Delta\delta D_{23\text{-}29}$ (mean 29‰) indicate a low evapo(transpi)ration due to lower temperatures and/or higher precipitation which is associated with higher lake levels and a higher effective moisture in the lake catchment. The moisture might have been carried along by stronger Westerlies and winter monsoon with partial melt-water input. In addition to U-shaped valleys with lateral moraines, drained rivers from Anyêmaqên foothills (~16 ± 3ka) provide evidence of former glaciation (IJmker et al., 2012b; Owen et al., 2003; Opitz et al., 2012). However, pollen data (Wang et al., 2014) from Lake Donggi Cona indicating an annual precipitation of about 200 mm, which is lower than today, may also indicate colder conditions and is in accordance with Lake Kuhai pollen record (Ji et al., 2005). Taking into account the dating uncertainties, the abrupt lowering of δD values of nC_{29} at ~15 cal ka BP may indicate rapid cooling which is consistent with the "Heinrich event 1" in the northern hemisphere (Broecker et al., 1992). In general, the climatic conditions during this interval were cold and moist with higher lake levels fed by fresh water from strong Westerlies rainfall as snow, continental moisture recycling and fluvial melt-water inflow into the lake.

5.3.1.2. Period 2 (3.7–2.2 m, 14.8–13.0 cal ka BP). This period can be characterized by variable environmental conditions and a very high mean sedimentation rate of about 94 cm/ka. The increase in the *n*-alkane amount of predominantly terrestrial plants and thus enhanced organic productivity implies warmer conditions. The CPI values (mean 26.6) are still quite high indicating the dominance of allochthonous/terrestrial organic matter. The higher input of terrestrial material in the lake basin might be a reason for the undisturbed laminations reflecting lake stratification and establishment of anoxia in the water column. High wind erosion rates together with low vegetation cover might have led to the high sediment accumulations. Higher values of $\delta^{13}C$ of nC_{23} as well as the abrupt rise in pyrite content during this episode (Opitz et al., 2012) indicate the stratified conditions causing disruption in the mixing of lake water that lead to the lowering of dissolved oxygen concentration in the water column. Although lake stratification hampers the growth of aquatic plants, mid-chain nC_{23} and Charafragments were found indicating minor presence of aquatic macrophytes (Aichner et al., 2012). Higher erosion rates are possibly attributed to the enhanced snow and permafrost melting due to higher temperature. However, higher mean δD values of nC_{23} (−124‰), nC_{29} (−146‰) indicate higher lake evaporation due to higher surface temperatures resulting in lower lake levels. The warm period at ~13.5 cal ka BP may be correlated to the North Atlantic Bølling-Allerød warm complex that has also been documented in nearby lake records such as Koucha, Kuhai and Qinghai (Ji et al., 2005; Shen et al., 2005a; Wischnewski et al., 2011; Zhang and Mischke, 2009). In general, the climatic conditions during this interval were warm with low effective moisture availability due to high evapo(transpi)ration rates and weaker summer monsoon and/or Westerlies.

5.3.1.3. Period 3 (2.2–1.4 m, 13.0–9.2 cal ka BP). The abrupt rise in the amount of *n*-alkanes is linked with an enhanced organic productivity favored by the early-Holocene increased insolation (Fig. 4). The decreasing trend in CPI (mean 12.0) and higher P_{aq} values (mean 0.31) reveal favorable conditions for the growth of macrophytes and, consequently, higher organic input into the lake. Lower mean δD values for nC_{23} (−140‰) and nC_{29} (−164‰) indicate an increasing lake level and higher summer precipitation representing climate optimum conditions. High amounts of precipitation outbalance the effect of rising temperatures resulting in higher moisture availability and depleted *n*-alkane δD values. Major source of moisture are the Westerlies and their summer precipitation. However, the northward migration of the intensified Asian monsoon systems in the early-Holocene can also contribute to the wetter conditions in the northern plateau (An et al., 2012b; Thompson et al., 2005; Wang et al., 2008; Zhao et al., 2007). In general, the climatic conditions during this interval were warm and humid with a lake high-stand at ~11.0 cal ka BP.

5.3.1.4. Period 4 (1.4–0.55 m, 9.2–3.0 cal ka BP). The abrupt decline in the amount of *n*-alkanes is marked with the major 8.2 ka cooling event in China (Liu et al., 2003; Wang et al., 2002). This cooling episode has been widely regarded as the most remarkable cooling episode during the Holocene (Jin et al., 2007). Later, the rise in organic productivity and increasing lake level as inferred from higher *n*-alkane amount and lower δD values of nC_{23} indicate humid conditions in the lake catchment. The effective moisture increased during mid-Holocene as evidenced by lower $\Delta\delta D_{C23\text{-}C29}$ values, while lower mean δD values of nC_{23} (−156‰) and nC_{29} (−186‰) also reflect higher moisture availability due to decreased evapo(transpi)ration and insolation (Marcott et al., 2013). However, during this period, although the summer monsoon weakened, the Westerlies probably carried major precipitation that lead to an increase in effective moisture, resulting in higher lake levels (Fig. 4). The lower CPI values (mean 11.4) and P_{aq} ratios (mean 0.18) indicate the input of fresh allochthonous/terrestrial organic matter into the lake. The higher mean effective moisture conditions have also been inferred by Herzschuh, 2006a during that episode. Similar conditions have also been reported in northern plateau from large lake such as Qinghai (Shen et al., 2005b), and other smaller lakes such as Lake An et Koucha (Herzschuh et al., 2009; Aichner et al., 2010b),

and Lake Sumxi (Gasse et al., 1991) and Lake Ximencuo (Zhang and Mischke, 2009) from western and eastern TP (Feng et al., 2006; Morrill et al., 2003; Zhou et al., 2002). In general, the climatic conditions during this interval were cold and humid with a high-stand at ~5.3 cal ka BP.

5.3.1.5. Period 5 (0.55–0.18 m, 3.0–1.2 cal ka BP). During the late-Holocene, Lake Donggi Cona continued to be a fresh water lake. Average total *n*-alkane concentration dropped compared to period 4 indicating a decline in organic productivity. This is accompanied by a lowering of the lake level as indicated by increasing lake evaporation inferred from higher mean δD values of nC_{23} (−143‰). The high CPI values (mean: 53.0) and the lowest P_{aq} values (mean: 0.14) suggest the dominance of terrestrial organic matter. However, the lower mean δD of nC_{29} (−179‰) and higher mean $\Delta\delta D_{23\text{-}29}$ (mean 47‰) suggest lower air temperatures but higher evapo(-transpi)ration rates and thus semi-arid conditions comparable to nowadays. Moreover higher $\delta^{18}O$ values from ostracods provide further evidence of colder conditions (Mischke et al., 2010a) in the Donggi Cona catchment. Near the top of the period, a sudden rise in *n*-alkane amounts is possibly related with the Medieval Warm Period (MWP) but might be also caused by increased human impact or dating uncertainties to some extent. There is no significant change in the vegetation type as inferred from relatively stable values of $\delta^{13}C$ for nC_{23} and nC_{29}. Therefore, in general, the conditions were colder and drier in the late-Holocene than in earlier period with moisture source predominantly from Westerlies and/or local moisture recycling sources. The Chinese Loess Plateau and Westerlies-influenced areas indicate similar trends of relatively dry late-Holocene between 4 and 0 cal ka BP (Chen et al., 2008; Lu et al., 2013). In general, the climatic conditions during this interval were colder and semi-arid except abrupt MWP ~1.6 ka BP.

5.4. Comparison with other records at the Tibetan Plateau

Although there are many lakes in the semi-arid region of the northeastern TP, multi-proxy paleoclimate data are still limited (Fig. 5). The nearest multi-proxy reconstructions were conducted in Lake Qinghai (ca. 230 km northeast) (Shen et al., 2005b; Thomas et al., 2016), Lake Koucha (ca. 200 km southwest) (Aichner et al., 2010b; Herzschuh et al., 2009), Lake Genggahai (ca. 250 km east) (Rao et al., 2014) and Lake Ximencuo (eastern TP) (Zhang and Mischke, 2009), whereas Lake Nam Co is located in south-central TP in the Asian monsoon controlled region (Mügler et al., 2010). The moisture availability in the Lake Donggi Cona catchment was significantly higher in the Late Glacial and early to mid-Holocene compared to the present day semi-arid conditions.

Our results show that between 18.4 and 14.8 cal ka BP, Lake Donggi Cona experienced cold and wet condition with high-stand at ~17 cal ka BP. This generally agrees with lake high-stands (~17.2–15.1 and/or ~16–14.9 cal ka) inferred from depleted δD_{wax} values from Lake Qinghai and Lake Chaka record (Liu et al., 2008, 2015; Thomas et al., 2016) and the existence of permanent deep-water Lake Naleng and Ximencuo ~17.7 cal ka BP (Graf et al., 2007; Zhang and Mischke, 2009). The existence of former glaciation in the north-western side of lake Donggi Cona catchment is apparently a prerequisite which maintained relatively high water levels during cold periods following the global LGM ~21 ka (Zhang and Mischke, 2009). However, Lake Koucha indicate rather, cold and dry climate (50% less precipitation than today) between 16.7 and 14.6 cal ka BP from its lake pollen spectra (Herzschuh et al., 2009). The GRIP ($\delta^{18}O$) record indicates relatively stable and wetter condition between 18.5 and 17.0 cal ka BP (Johnsen et al., 2001). Considering the dating uncertainties in our record, the reversal from wet to dry conditions may coincide with the “Heinrich 1” event in the North-Atlantic (Broecker et al., 1992). An et al. (2012), reported that the Qinghai Lake catchment might have experienced similar conditions due to decreased oceanic moisture transport during the Late Glacial period. This might have led to the dominance of continental air masses and moisture recycling processes. This indicates that the moisture source might have been predominantly Westerlies and melt-water input from adjacent glaciers. Similarly cold and wet conditions have also been deduced from the Westerly influenced Lake Qinghai and Chinese Loess records based on pollen concentrations, carbonates and TOC values in this period (An et al., 2012b; Vandenberghe et al., 2006).

Warm and arid conditions prevailed in the Donggi Cona catchment between 14.8 and 13.0 cal ka BP. The low vegetation cover in the catchment along with rising temperature and therefore enhanced permafrost melting in the region might have favored the transportation of terrestrial material into the lake that lead to high SAR. Similarly, Mischke et al. (2008) inferred the presence of black layers and high TOC in the Lake Koucha record to be representative of shallow, hypersaline and anoxic lake conditions. This overall pattern dictates the strong evapo(transpi)ration conditions, which probably restrain the moisture availability to the northeastern TP, followed by strengthening of the summer monsoon in the early-Holocene. Variably, but in general, higher $\delta^{18}O$ values from the Guliya ice core between 14.6 and 13.0 cal ka BP marks higher temperatures on the northwestern TP (Thompson et al., 1997). During the Bølling-Allerød period at ~14.5 cal ka BP, rising temperatures in northern hemisphere lead to northward shifting of Westerlies and the ITCZ (Denton, 2010) which is in agreement with the abrupt decline in pollen concentration (due to decline in precipitation driven pollens) from Lake Koucha and Kuhai (Herzschuh et al., 2009; Wischnewski et al., 2011) during that episode. This is consistent with higher δD values (of nC_{23} and nC_{29}) which indicate warm and arid condition from Lake Koucha (Rao et al., 2014). Also the increasing $\delta^{13}C$ values δD_{wax} in Lake Qinghai (Thomas et al., 2014, 2016) indicate probably enhanced aquatic productivity indicating warmer and more arid conditions. Lake Genggahai indicated to be at low lake levels until ~11.4 cal ka (Qiang et al., 2013) due to arid conditions. The abrupt increase in TOC in Lake Ximencou probably reflects the warming that correlates with the Bølling-Allerød seen in the NGRIP and GRIP ice cores (Lowe et al., 2008). This suggests that the general warming decreased the intensity of the Westerlies which reduced the moisture transport and increased arid conditions during that episode.

Between 13.0 and 9.2 cal ka BP, the Lake Donggi Cona experienced early-Holocene warm and humid conditions. This period marks a lake high-stand ~11 cal ka BP and significantly higher summer precipitation. Several other lakes from eastern margin of TP also reported higher lake levels during that period (Hong et al., 2003; Zhou et al., 2002). Warm and humid conditions were also revealed from Lake Kuhai records based on ostracod assemblages (Mischke et al., 2010d). Higher $\delta^{18}O$ values in the Guliya ice core during this period also give evidence for warm conditions on the northwestern TP (Thompson et al., 1997). Lake Donggi Cona catchment indicates no significant increase in C_4 plants as indicated in Lake Qinghai. The lower resolution, smaller size and significant mixing of the water column may impede the detection of this short interval of moisture change as shown in Lake Qinghai (Thomas et al., 2016; Aichner et al., 2012). Lake Qinghai indicates a warm climate from early to mid-Holocene based on lighter δD_{wax} valves, higher pollen concentration, carbonate content and TOC values, indicating a rise in temperature and precipitation during 10.8–4.5 cal ka BP (Shen et al., 2005b; Thomas et al., 2016). This correlates well with higher *n*-alkane amounts, wetter conditions and higher lake levels in Lake Donggi Cona during that time (Dietze et al., 2013). This reconstruction is consistent with the prevailing

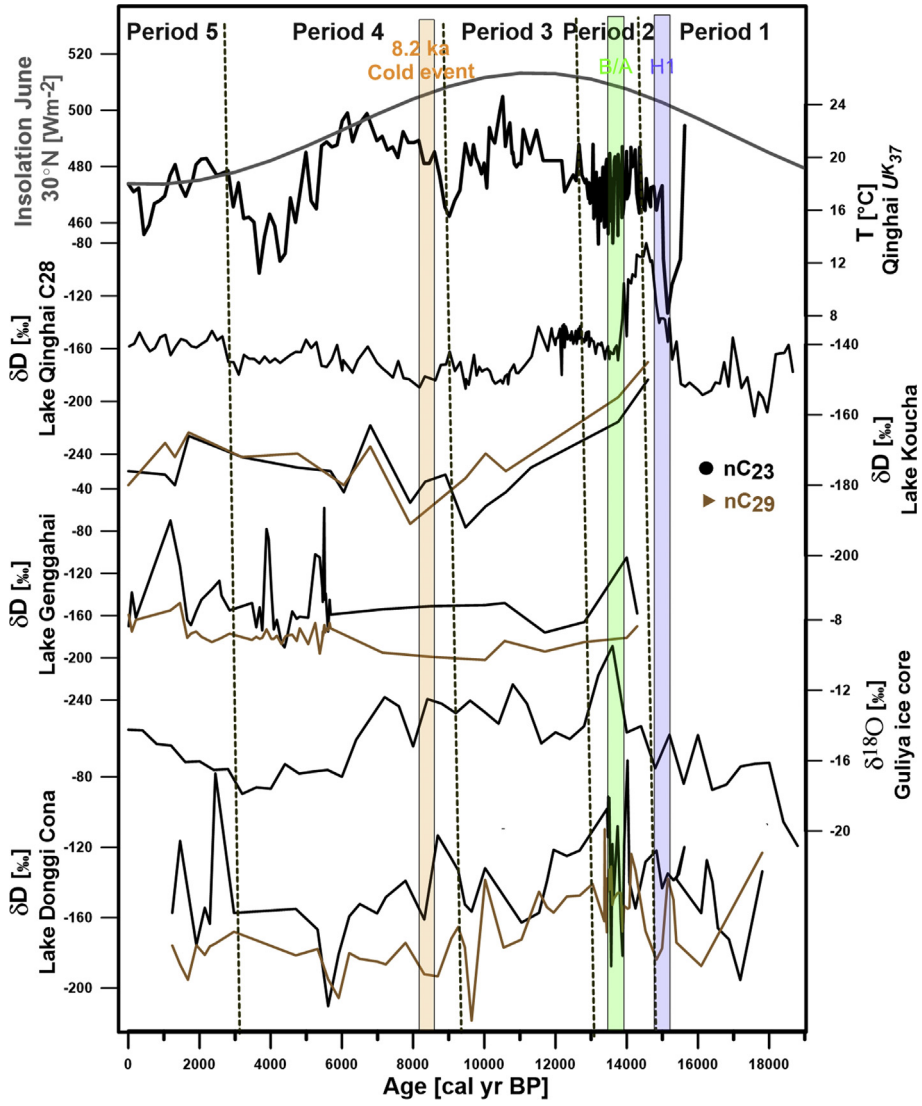

Fig. 5. Comparison of δD record with $\delta^{18}O$ record of Guliya ice core (Thompson et al., 1997), δD record from lakes Genggahai (Rao et al., 2014), Lake Koucha (Aichner et al., 2010a) and The δD_{wax} curve is based on Lake Qinghai core (Thomas et al., 2016). Alkenone based temperature record (U^{K}_{37}) from Lake Qinghai (Hou et al., 2016) whereas solar insolation at 30°N in June (Berger and Loutre, 1991) are shown on the top.

view that summer monsoon intensified during this period which resulted in a substantial increase in precipitation (An et al., 2012b). Between 13.0 and 9.2 cal ka BP, the Lake Donggi Cona experienced early-Holocene warm and humid conditions. This period marks a lake high-stand ~11 cal ka BP and significantly higher summer precipitation. Several other lakes from eastern margin of TP also reported higher lake levels during that period (Hong et al., 2003; Zhou et al., 2002). Warm and humid conditions were also revealed from Lake Kuhai records based on ostracod assemblages (Mischke et al., 2010d). Higher $\delta^{18}O$ values in the Guliya ice core during this period also give evidence for warm conditions on the northwestern TP (Thompson et al., 1997). Lake Donggi Cona catchment indicates no significant increase in C_4 plants as shown by stable $\delta^{13}C$ values of terrestrial compounds in this core (Aichner et al., 2012, Fig. 4). This is in agreement with proxy and modeling inferences that C_4-plants have been absent on the Tibetan Plateau during the past 20 ka (Berling and Woodward, 2001) but contradicts Thomas et al. (2014) who suggested the abundance of C_4-plants in the Lake Qinghai catchment between 14 and 6 ka. Lake Qinghai indicates a warm climate from early to mid-Holocene based on lighter δD_{wax} values, higher pollen concentration, carbonate content and TOC values, indicating a rise in temperature and precipitation during 10.8–4.5 cal ka BP (Shen et al., 2005b; Thomas et al., 2016). This correlates well with higher *n*-alkane amounts, wetter conditions and higher lake levels in Lake Donggi Cona during that time (Dietze et al., 2013). This reconstruction is consistent with the prevailing view that summer monsoon intensified during this period which resulted in a substantial increase in precipitation (An et al., 2012b).

In the mid-Holocene (between 9.2 and 3.0 cal ka BP), however, lake evaporation decreased as temperature dropped, resulted in high effective moisture availability and another lake high-stand at ~5.3 cal ka BP. This pattern generally agrees with the wet condition inferred between 7 and 4.5 cal ka BP from lake pollen spectra (Wang et al., 2014). This period is characterized by lower temperatures, annual precipitation of about ~340 mm and higher lake levels (lighter δD values) compared to the early-Holocene (Wang et al., 2014). This wet period is generally synchronous with the intensified Asian summer monsoon, displayed by many moisture records from monsoonal central Asia (Wang et al., 2010) and

Westerly influenced, Chinese Loess Plateau (Chen et al., 2008; Lu et al., 2013). Similarly, Lake Nam Co in the central TP indicates humid climate conditions with intense precipitation and potential melt-water input into the lake catchment in this period (Mügler et al., 2008). Lake Donggi Cona during this period experienced reduced evaporative conditions due to decreased insolation in Northern Hemisphere as shown by other records from Donggi Cave and Arabian sea (Overpeck et al., 1996; Wang et al., 2005). The cold event between 7.9 and 7.4 cal ka BP from Lake Ximencuo was recorded at a number of sites on the eastern TP, too and probably corresponds to the cold event ~8.2 cal ka BP which is also visible at other sites on TP (Mischke and Zhang, 2010c; Zhang and Mischke, 2009). δD_{wax}, alkenone based temperature record from Lake Qinghai indicates cooling as well as weekend summer monsoon in this interval (Hou et al., 2016; Thomas et al., 2016). However, ^{14}C, OSL ages and stratigraphic interpretations from Lake Qinghai indicate the highest lake-stand during the Holocene at 7.4–6.0 cal ka BP and 8.0–5.0 cal ka BP (Liu et al., 2015). Similarly, high lake levels in Genggahai Lake (Rao et al., 2014) occurred at 7.4–6.3 cal ka BP (Qiang et al., 2013).

In the late-Holocene during 3.0–1.2 ka BP, Lake Donggi Cona remained an oligotrophic well ventilated fresh water lake with steadily dry conditions and enhanced aeolian input (Dietze et al., 2015; IJmker et al., 2012b). Average total *n*-alkane concentration is lower than in period 4. This decline in biological productivity is also accompanied by lowering of lake levels as indicated by higher δD values of nC_{23}. Lower δD values of nC_{29} indicate lower temperatures and a weakening of summer precipitation. Lower $\delta^{18}O$ values in the Guliya ice core during this period also give evidence for colder conditions on the northwestern TP (Thompson et al., 1997). The abrupt rise in biological productivity with higher *n*-alkanes amount may possibly coincide with MWP. Although, the higher $\delta^{18}O$ values from ostracod assemblages provide further evidence of colder climate (Mischke et al., 2010a). Relatively low biomarker concentrations and $\delta^{13}C$ values at 3.1 and 1.8 cal ka BP indicate the occurrence of cool periods in Lake Koucha (Aichner et al., 2010b). Lake Qinghai indicate a decline in lake levels from ~4 to 3 and ~2-0 cal ka BP and, therefore, indicate cold and semi-arid conditions based upon coarse grain size, very low carbonate and heavier $n\text{-}C_{28}$ δD_{wax} (Liu et al., 2002, 2015; Thomas et al., 2016) as well as decline in pollen, aragonite, TOC and TN and shoreline dating (Ji et al., 2005). Lake Ximencuo, also reflect cold and dry conditions during 3.6–0 cal ka BP based on pronounced maxima in the χ_{FD} values which reflect the influx of pedogenic magnetite/maghemite grains (Zhang and Mischke, 2009). However, lake records from the southern TP, i.e. Nam Co, also indicate cold and drier conditions with lower lake levels during this period (Mügler et al., 2008). A decline in moisture availability has been inferred between 4.5 and 2.0 cal ka BP from Lake Kuhai (Wischnewski et al., 2011) and many other records from the TP and Asia (An, 2006; Mischke et al., 2010d; Mügler et al., 2010; Morrill et al., 2006; Shen et al., 2005b). The modern circulation with dominating influence of the Westerlies combined with local moisture recycling was established ~3 ka as indicated by our proxy record.

6. Conclusion

Our records support the previously reconstructed hydroclimatic changes on northeastern TP with deuterium depletion starting at ca. 14–15 ka driven by a major change of moisture source at the glacial to the Holocene transition. Further, stable carbon isotopic values of ca. −32‰ give evidence for the absence of C_4-vegetation in the lake catchment throughout the studied interval. Lake Donggi Cona has been a permanent deep lake existed since at least 19 cal ka BP. In the early existence of a lake, the basin was probably fed by glacier melt-water following the LGM indicating a sensitive response to the onset of slight warming. We suggest that lake levels at ~16.9, ~11.0 and ~5.3 cal ka BP were higher than at present, while the lake level continuously declined in the last 5 ka. Sediments of Lake Donggi Cona were, in general, macrophyte dominated before 14.8 cal ka BP, and later shifted to be dominated by terrestrial plants and grasses. We propose that the climatic conditions were cold and moist with higher lake levels between 19 and 14.8 cal ka BP due to enhanced moisture availability coming from ever stonger Westerlies, Winter air masses and melt-water from adjacent glaciated mountains. Higher temperature and arid conditions followed during 14.8–13 ka BP associated with the Bølling-Allerød warm complex. High evaporative condition in this period resulted in lowest lake stand and thus an arid climate due to waning Westerlies and slight strengthening of the summer monsoon which we propose was the predominant moisture source during Bølling-Allerød and the early-Holocene. Increased terrestrial input demonstrates the transition from Late Glacial to Holocene that has been identified in many lacustrine records in the TP following a trend of increasing Northern Hemisphere summer insolation. During 9.2–3.0 cal ka BP, Westerlies and moisture recycling brought most of the moisture following reduced insolation in Northern Hemisphere that lead to high moisture availability. Since ~3 ka, the lake has been a fresh-water, oligotrophic lake and experienced colder and semi-arid conditions with moisture from Westerlies and moisture recycling. The input of terrestrial organic matter gradually increased from the early Holocene, interrupted by a period of lower biomarker concentrations which was possibly triggered by cool and arid conditions between ca. 3.5 to 1.7 cal ka BP. The Lake Donggi Cona δD and $\delta^{13}C$ record highlights the advantage of organic geochemical proxies to infer paleohydrological and -ecological changes that are not covered by other proxies on the Tibetan Plateau.

Acknowledgements

We would like to thank German Research Foundation (DFG) for funding within the priority program 1372 “Tibetan Plateau: Formation – Climate – Ecosystems (TiP)” and of project Ai 134/2–1, GL 262/16. This study is a joint cooperation with the Institute of Tibetan Plateau Research. We also want to thank Roman Witt, Steffen Rühlow and Elisabeth Dietze for assistance, MPI for Biogeochemistry, IMPRS gBGC and Institute of Geography, FSU-Jena for additional project funding in the framework of the TiP.

References

Aichner, B., Herzschuh, U., Wilkes, H., Vieth, A., Böhner, J., 2010a. δD values of n-alkanes in Tibetan lake sediments and aquatic macrophytes - a surface sediment study and application to a 16 ka record from Lake Koucha. Org. Geochem. 41, 779–790.

Aichner, B., Wilkes, H., Herzschuh, U., Mischke, S., Zhang, C.J., 2010b. Biomarker and compound-specific $\delta^{13}C$ evidence for changing environmental conditions and carbon limitation at Lake Koucha, eastern Tibetan Plateau. J. Paleolimnol. 43, 873–899.

Aichner, B., Herzschuh, U., Wilkes, H., 2010c. Influence of aquatic macrophytes on the stable carbon isotopic signatures of sedimentary organic matter in lakes on the Tibetan Plateau. Org. Geochem. 41, 706–718.

Aichner, B., Herzschuh, U., Wilkes, H., Schulz, H.M., Wang, Y.B., Plessen, B., Mischke, S., Diekmann, B., Zhang, C.J., 2012. Ecological development of Lake Donggi Cona, north-eastern Tibetan Plateau, since the late glacial on basis of organic geochemical proxies and non-pollen palynomorphs. Palaeogeogr. Palaeoclimatol. Palaeoecol. 313, 140-(Thomas et al., 2014)149.

Allen, E.D., Spence, D.H.N., 1981. The differential ability of aquatic plants to utilize the inorganic carbon supply in fresh water. New Phytol. 87, 269–283.

An, C.-B., Lu, Y., Zhao, J., Tao, S., Dong, W., Li, H., Jin, M., Wang, Z., 2012a. A high-resolution record of Holocene environmental and climatic changes from Lake Balikun (Xinjiang, China): implications for central Asia. Holocene 22, 43–52.

An, Z., Porter, S.C., Kutzbach, J.E., Xihao, W., Suming, W., Xiaodong, L., Xiaoqiang, L., Weijian, Z., 2000. Asynchronous Holocene optimum of the east Asian monsoon. Quat. Sci. Rev. 19, 743–762.

An, Z.S., 2000. The history and variability of the East Asian paleomonsoon climate. Quat. Sci. Rev. 19, 171–187.
An, Z.S., 2006. Geophysical survey on the tectonic and sediment distribution of Qinghai Lake basin. Sci. China (Series D Earth Sci. 49, 851–861.
An, Z.S., Colman, S.M., Zhou, W.J., Li, X.Q., Brown, E.T., Jull, A.J.T., Cai, Y.J., Huang, Y.S., Lu, X.F., Chang, H., Song, Y.G., Sun, Y.B., Xu, H., Liu, W.G., Jin, Z.D., Liu, X.D., Cheng, P., Liu, Y., Ai, L., Li, X.Z., Liu, X.J., Yan, L.B., Shi, Z.G., Wang, X.L., Wu, F., Qiang, X.K., Dong, J.B., Lu, F.Y., Xu, X.W., 2012b. Interplay between the Westerlies and Asian monsoon recorded in lake Qinghai sediments since 32 ka. Sci. Rep. UK 2, 619.
Araguas-Araguas, L., Froehlich, K., Rozanski, K., 1998. Stable isotope composition of precipitation over southeast Asia. J. Geophys. Res. Atmos. 103, 28721–28742.
Berling, D.J., Woodward, F.I., 2001. Vegetation and the Terrestrial Carbon Cycle. Cambridge University Press, Cambridge, UK, pp. 303–324.
Berger, A., Loutre, M.F., 1991. Insolation values for the climate of the past 10 million years. Quat. Sci. Rev. 10, 297–317.
Bray, E.E., Evans, E.D., 1961. Distribution of normal-parafines as a clue to recognition of source beds. Geochim. Cosmochim. Acta 22, 2–15.
Broecker, W., Bond, G., Klas, M., Clark, E., McManus, J., 1992. Origin of the northern Atlantic's Heinrich events. Clim. Dyn. 6, 265–273.
Chen, F.H., Zhu, Y., Li, J.J., Shi, Q., Jin, L.Y., Wünemann, B., 2001. Abrupt Holocene changes of the Asian monsoon at millennial- and centennial-scales: evidence from lake sediment document in Minqin Basin, NW China. Chin. Sci. Bull. 46, 1942–1947.
Chen, F.H., Holmes, J.A., 2003. Multi-proxy evidence for late Pleistocene-Holocene environmental change in and Central Asia: an overview of the RACHAD 2001 symposium. Chin. Sci. Bull. 48, 1397–1400.
Chen, F.-H., Cheng, B., Zhao, Y., Zhu, Y., Madsen, D.B., 2006. Holocene environmental change inferred from a high-resolution pollen record, Lake Zhuyeze, arid China. Holocene 16, 675–684.
Chen, F., Yu, Z., Yang, M., Ito, E., Wang, S., Madsen, D.B., Huang, X., Zhao, Y., Sato, T., Birks, H.J.B., Boomer, I., Chen, J., An, C., Wünnemann, B., 2008. Holocene moisture evolution in arid central Asia and its out-of-phase relationship with Asian monsoon history. Quat. Sci. Rev. 27, 351–364.
Denton, G.H., 2010. The last glacial termination. Science 328, 1652–1656.
Dietze, E., Wünnemann, B., Diekmann, B., Aichner, B., Hartmann, K., Herzschuh, U., IJmker, J., Jin, H., Kopsch, C., Lehmkuhl, F., Li, S., Mischke, S., Niessen, F., Opitz, S., Stauch, G., Yang, S., 2010. Basin morphology and seismic stratigraphy of lake Donggi Cona, north-eastern Tibetan Plateau, China. Quat. Int. 218, 131–142.
Dietze, E., Wünnem ann, B., Hartmann, K., Diekmann, B., Jin, H., Stauch, G., Yang, S., Lehmkuhl, F., 2013. Early to mid-Holocene lake high-stand sediments at lake Donggi Cona,northeastern Tibetan Plateau, China. Quat. Res. 79, 325e 336.
Dietze, E., Lockot, G., Hartmann, K., Lehmkuhl, F., Stauch, G., Wünnemann, B., 2015. Early to mid-Holocene lake high-stand sediments at Lake Donggi Cona, northeastern Tibetan Plateau, China-Response to comments by Mischke et al. Quat. Res. 79 (3), 325–336. Quaternary Research 83, 259–260.
Eglinton, G., Hamilton, R.J., 1967. Leaf epicuticular waxes. Science 156, 1322.
Feng, Z.D., An, C.B., Wang, H.B., 2006. Holocene climatic and environmental changes in the arid and semi-arid areas of China: a review. Holocene 16, 119–130.
Ficken, K.J., Li, B., Swain, D.L., Eglinton, G., 2000. An n-alkane proxy for the sedimentary input of submerged/floating freshwater aquatic macrophytes. Org. Geochem. 31, 745–749.
Gasse, F., Arnold, M., Fontes, J.C., Fort, M., Gibert, E., Huc, A., Li, B.Y., Li, Y.F., Lju, Q., Melieres, F., Vancampo, E., Wang, F.B., Zhang, Q.S., 1991. A 13,000-year climate record from Western Tibet. Nature 353, 742–745.
Gat, J.R., 1996. Oxygen and hydrogen isotopes in the hydrologic cycle. Annu. Rev. Earth Planet. Sci. 24, 225–262.
Gao, L., Hou, J.Z., Toney, J., MacDonald, D., Huang, Y., 2011. Mathematical modelling of the aquatic macrophyte inputs of mid-chain n-alkyl lipids to lake sediments: implications for interpreting compound-specific hydrogen isotopic records. Geochem. Cocmochim. Acta 75, 3781–3791.
Gehre, M., Geilmann, H., Richter, J., Werner, R.A., Brand, W.A., 2004. Continuous flow H-2/H-1 and and(18)O/O-16 analysis of water samples with dual inlet precision. Rapid Commun. Mass Spectrom. 18, 2650–2660.
Graf, A., Strasky, S., Zhao, Z., Ivy-Ochs, S., Kubik, P.W., Baur, H.W., Wieler, R., Schlüchter, C., 2007. Cosmogenic nuclides concentrations indicate an ice advance during MIS-2 in the monsoon influenced Shaluli Mountains, eastern Tibet. Quat. Int. 167–168, 485.
Günther, F., Aichner, B., Siegwolf, R., Xu, B., Yao, T., Gleixner, G., 2013. A synthesis of hydrogen isotope variability and its hydrological significance at the Qinghai-Tibetan Plateau. Quat. Int. 313, 3–16.
Günther, F., Witt, R., Schouten, S., Mäusbacher, R., Daut, G., Zhu, L., Xu, B., Yao, T., Gleixner, G., 2015. Quaternary ecological responses and impacts of the indian ocean summer monsoon at Nam Co, Southern Tibetan Plateau. Quart. Sci. Rev. 112, 66–77.
Hartmann, K., Wünnemann, B., 2009. Hydrological changes and Holocene climate variations in NW China, inferred from lake sediments of Juyanze palaeolake by factor analyses. Quat. Int. 194, 28–44.
Herzschuh, U., Tarasov, P., Wünnemann, B., Hartmann, K., 2004. Holocene vegetation and climate of the Alashan Plateau, NW China, reconstructed from pollen data. Palaeogeogr. Palaeoclimatol. Palaeoecol. 211, 1–17.
Herzschuh, U., 2006a. Palaeo-moisture evolution in monsoonal Central Asia during the last 50,000 years. Quat. Sci. Rev. 25, 163–178.
Herzschuh, U., Kürschner, H., Mischke, S., 2006b. Temperature variability and vertical vegetation belt shifts during the last similar to 50,000 yr in the Qilian Mountains (NE margin of the Tibetan Plateau, China). Quat. Res. 66, 133–146.
Herzschuh, U., Kramer, A., Mischke, S., Zhang, C., 2009. Quantitative climate and vegetation trends since the late glacial on the northeastern Tibetan Plateau deduced from Koucha Lake pollen spectra. Quat. Res. 71, 162–171.
Hong, Y.T., Hong, B., Lin, Q.H., Zhu, Y.X., Shibata, Y., Hirota, M., Uchida, M., Leng, X.T., Jiang, H.B., Xu, H., Wang, H., Yi, L., 2003. Correlation between Indian Ocean summer monsoon and North Atlantic climate during the Holocene. Earth Planet. Sci. Lett. 211, 371–380.
Hou, J.Z., Huang, Y.S., Zhao, J.T., Liu, Z.H., Colman, S., An, Z.S., 2016. Large Holocene summer temperature oscillations and impact on the peopling of the north-eastern Tibetan Plateau. Geophys. Res. Lett. 43, 1323–1330.
Huang, Y.S., Shuman, B., Wang, Y., Webb, T., 2004. Hydrogen isotope ratios of individual lipids in lake sediments as novel tracers of climatic and environmental change: a surface sediment test. J. Paleolimnol. 31, 363–375.
IJmker, J., Stauch, G., Poetsch, S., Diekmann, B., Wünnemann, B., Lehmkuhl, F., 2012a. Dry periods on the NE Tibetan Plateau during the late quaternary. Palaeogeogr. Palaeoclimatol. Palaeoecol. 346, 108–119.
IJmker, J., Stauch, G., Dietze, E., Hartmann, K., Diekmann, B., Lockot, G., Opitz, S., Wünnemann, B., Lehmkuhl, F., 2012b. Characterisation of transport processes and sedimentary deposits by statistical end-member mixing analysis of terrestrial sediments in the Donggi Cona lake catchment, NE Tibetan Plateau. Sediment. Geol. 281, 166–179.
Ji, S., Xingqi, L., Sumin, W., Matsumoto, R., 2005. Palaeoclimatic changes in the Qinghai Lake area during the last 18,000 years. Quat. Int. 136, 131–140.
Jin, Z.D., Yu, J., Chen, H.X., Wu, Y.H., Wang, S.M., Chen, S.Y., 2007. The influence and chronological uncertainties of the 8.2 ka cooling event on continental climate records in China. Holocene 17, 1041–1050.
Johnsen, S.J., DahlJensen, D., Gundestrup, N., Steffensen, J.P., Clausen, H.B., Miller, H., Masson-Delmotte, V., Sveinbjornsdottir, A.E., White, J., 2001. Oxygen isotope and palaeotemperature records from six Greenland ice-core stations: camp Century, Dye-3, GRIP, GISP2, Renland and NorthGRIP. J. Quat. Sci. 16, 299–307.
Kang, S., Xu, Y., You, Q., Flügel, W.-A., Pepin, N., Yao, T., 2010. Review of climate and cryospheric change in the Tibetan Plateau. Environ. Res. Lett. 5.
Kürschner, H., Herzschuh, U., Wagner, D., 2005. Phytosociological studies in the north-eastern Tibetan Plateau (NW China) - a first contribution to the subalpine scrub and alpine meadow vegetation. Bot. Jahrbücher für Syst. Pflanzengesch. Pflanzengeogr. 126, 273–315.
Liu, C.L., Wang, M.L., Jiao, P.C., Li, S., Chen, Y.Z., 2003. Holocene yellow silt layers and the paleoclimate event of 8200 a BP in Lop Nur, Xinjiang, NW China. Acta Geol. Sin. Engl. Ed. 77, 514–518.
Liu, X.J., Lai, Z., Madsen, D., Zeng, F., 2015. Last deglacial and Holocene lake level variations of Qinghai Lake, north-eastern Qinghai-Tibetan Plateau. J. Quat. Sci. 30, 245–257.
Liu, X.Q., Shen, J., Wang, S.M., Yang, X.D., Tong, G.B., Zhang, E.L., 2002. A 16000-year pollen record of Qinghai Lake and its paleoclimate and paleoenvironment. Chin. Sci. Bull. 47, 1931–U1936.
Liu, X., Dong, H., Rech, J.A., Matsumoto, R., Bo, Y., Wang, Y., 2008. Evolution of Chaka salt lake in NW China in response to climatic change during the latest Pleistocene-Holocene. Quat. Sci. Rev. 27, 867–879.
Long, H., Shen, J., Tsukamoto, S., Chen, J., Yang, L., Frechen, M., 2014. Dry early Holocene revealed by sand dune accumulation chronology in Bayanbulak Basin (Xinjiang, NW China). Holocene 24, 614–626.
Lowe, J.J., Rasmussen, S.O., Björck, S., Hoek, W.Z., Steffensen, J.P., Walker, M.J.C., Yu, Z.C., Grp, I., 2008. Synchronisation of palaeoenvironmental events in the North Atlantic region during the Last Termination: a revised protocol recommended by the INTIMATE group. Quat. Sci. Rev. 27, 6–17.
Lu, H., Yi, S., Liu, Z., Mason, J.A., Jiang, D., Cheng, J., Stevens, T., Xu, Z., Zhang, E., Jin, L., Zhang, Z., Guo, Z., Wang, Y., Otto-Bliesner, B., 2013. Variation of East Asian monsoon precipitation during the past 21 k.y. and potential CO_2 forcing. Geology 41, 1023–1026.
Ma, J., Edmunds, W.M., He, J., Jia, B., 2009. A 2000 year geochemical record of palaeoclimate and hydrology derived from dune sand moisture. Palaeogeogr. Palaeoclimatol. Palaeoecol. 276, 38–46.
Marcott, S.A., Shakun, J.D., Clark, P.U., Mix, A.C., 2013. A reconstruction of regional and global Temperature for the Past 11,300 Years. Science 339, 1198–1201.
Meyers, P.A., 2003. Applications of organic geochemistry to paleolimnological reconstructions: a summary of examples from the Laurentian Great Lakes. Org. Geochem. 34, 261–289.
Meyers, P.A., Ishiwatari, R., 1993. Lacustrine organic geochemistry - an overview of indicators of organic-matter sources and diagenesis in Lake-sediments. Org. Geochem. 20, 867–900.
Meyers, P.A., Lallier-Verges, E., 1999. Lacustrine sedimentary organic matter records of Late Quaternary paleoclimates. J. Paleolimnol. 21, 345–372.
Mischke, S., Kramer, M., Zhang, C., Shang, H., Herzschuh, U., Erzinger, J., 2008. Reduced early Holocene moisture availability in the Bayan Har Mountains, northeastern Tibetan Plateau, inferred from a multi-proxy lake record. Palaeogeogr. Palaeoclimatol. Palaeoecol. 267, 59–76.
Mischke, S., Aichner, B., Diekmann, B., Herzschuh, U., Plessen, B., Wünnemann, B., Zhang, C., 2010a. Ostracods and stable isotopes of a late glacial and Holocene lake record from the NE Tibetan Plateau. Chem. Geol. 276, 95–103.
Mischke, S., Zhang, C., 2010c. Holocene cold events on the Tibetan Plateau. Glob. Planet. Change 72, 155–163.
Mischke, S., Zhang, C., Börner, A., Herzschuh, U., 2010d. Lateglacial and Holocene variation in aeolian sediment flux over the northeastern Tibetan Plateau recorded by laminated sediments of a saline meromictic lake. J. Quat. Sci. 25,

162–177.
Morrill, C., Overpeck, J.T., Cole, J.E., 2003. A synthesis of abrupt changes in the Asian summer monsoon since the last deglaciation. Holocene 13, 465–476.
Morrill, C., Overpeck, J.T., Cole, J.E., Liu, K.B., Shen, C.M., Tang, L.Y., 2006. Holocene variations in the Asian monsoon inferred from the geochemistry of lake sediments in central Tibet. Quat. Res. 65, 232–243.
Mügler, I., Sachse, D., Werner, M., Xu, B., Wu, G., Yao, T., Gleixner, G., 2008. Effect of lake evaporation on δD values of lacustrine n-alkanes: a comparison of Nam Co (Tibetan Plateau) and Holzmaar (Germany). Org. Geochem. 39, 711–729.
Mügler, I., Gleixner, G., Günther, F., Mäusbacher, R., Daut, G., Schütt, B., Berking, J., Schwalb, A., Schwark, L., Xu, B., Yao, T., Zhu, L., Yi, C., 2010. A multi-proxy approach to reconstruct hydrological changes and Holocene climate development of Nam Co, Central Tibet. J. Paleolimnol. 43, 625–648.
Oleary, M.H., 1988. Carbon isotopes in photosynthesis. Bioscience 38, 328–336.
Opitz, S., Wünnemann, B., Aichner, B., Dietze, E., Hartmann, K., Herzschuh, U., IJmker, J., Lehmkuhl, F., Li, S., Mischke, S., Plotzki, A., Stauch, G., Diekmann, B., 2012. Late glacial and Holocene development of lake Donggi Cona, northeastern Tibetan Plateau, inferred from sedimentological analysis. Palaeogeogr. Palaeoclimatol. Palaeoecol. 337, 159–176.
Overpeck, J., Anderson, D., Trumbore, S., Prell, W., 1996. The southwest Indian Monsoon over the last 18000 years. Clim. Dyn. 12, 213–225.
Owen, L.A., Finkel, R.C., Haizhou, M., Spencer, J.Q., Derbyshire, E., Barnard, P.L., Caffee, M.W., 2003. Timing and style of late quaternary glaciation in northeastern Tibet. Geol. Soc. Am. Bull. 115, 1356–1364.
Pagani, M., Pedentchouk, N., Huber, M., Sluijs, A., Schouten, S., Brinkhuis, H., Damste, J.S.S., Dickens, G.R., Jakobsson, M., Expedition, S., 2006. Arctic hydrology during global warming at the Palaeocene/Eocene thermal maximum. Nature 443, 598–598.
Poynter, J., Eglinton, G., 1990. Moleculare composition of sediments from ODP Hole 116-717C. Pangaea. http://dx.doi.org/10.1594/PANGAEA.756551.
Pu, Z.-h., Zhang, Y.-q., Yin, Z.-q., Xu, J., Jia, R.-y., Lu, Y., Yang, F., 2010. Antibacterial activity of 9-octadecanoic acid-Hexadecanoic acid-Tetrahydrofuran-3,4-diyl ester from neem oil. Agric. Sci. China 9, 1236–1240.
Qiang, M., Song, L., Chen, F., Li, M., Liu, X., Wang, Q., 2013. A 16-ka lake-level record inferred from macrofossils in a sediment core from Genggahai Lake, northeastern Qinghai-Tibetan Plateau (China). J. Paleolimnol. 49, 575–590.
Qin, D., Xiao, C., 2009. Global climate change and cryospheric evolution in China. In: Boutron, C. (Ed.), Erca: from the Human Dimensions of Global Environmental Change to the Observation of the Earth from Space, vol. 8, pp. 19–28.
Rao, Z., Jia, G., Qiang, M., Zhao, Y., 2014. Assessment of the difference between mid- and long chain compound specific δD n-alkanes values in lacustrine sediments as a paleoclimatic indicator. Org. Geochem. 76, 104–117.
Ren, W., Yao, T., Yang, X., Joswiak, D.R., 2013. Implications of variations in $\delta^{18}O$ and δD in precipitation at Madoi in the eastern Tibetan Plateau. Quat. Int. 313, 56–61.
Sachse, D., Radke, J., Gleixner, G., 2006. δD values of individual n-alkanes from terrestrial plants along a climatic gradient - implications for the sedimentary biomarker record. Org. Geochem. 37, 469–483.
Shen, J., Liu, X.Q., Matsumoto, R., Wang, S.M., Yang, X.D., 2005a. A high-resolution climatic change since the Late Glacial Age inferred from multi-proxy of sediments in Qinghai Lake. Sci. China Ser. D Earth Sci. 48, 742–751.
Shen, J., Liu, X.Q., Wang, S.M., Matsumoto, R., 2005b. Palaeoclimatic changes in the Qinghai Lake area during the last 18,000 years. Quat. Int. 136, 131–140.
Thomas, E.K., Huang, Y.S., Morrill, C., Zhao, J.T., Wegener, P., Clemens, S.C., Colman, S.M., Gao, L., 2014. Abundant C-4 plants on the Tibetan Plateau during the lateglacial and early Holocene. Quat. Sci. Rev. 87, 24–33.
Thomas, E.K., Huang, Y.S., Clemens, S.C., Colman, S.M., Morrill, C., Wegener, P., Zhao, J.T., 2016. Changes in dominant moisture sources and the consequences for hydroclimate on the northeastern Tibetan Plateau during the past 32 kyr. Quat. Sci. Rev. 131, 157–167.
Thompson, L.G., Yao, T., Davis, M.E., Henderson, K.A., MosleyThompson, E., Lin, P.N., Beer, J., Synal, H.A., ColeDai, J., Bolzan, J.F., 1997. Tropical climate instability: The last glacial cycle from a Qinghai-Tibetan ice core. Science 276, 1821–1825.
Thompson, L.G., Davis, M.E., Mosley-Thompson, E., Lin, P.N., Henderson, K.A., Mashiotta, T.A., 2005. Tropical ice core records: evidence for asynchronous glaciation on Milankovitch timescales. J. Quat. Sci. 20, 723–733.
Tian, L., Masson-Delmotte, V., Stievenard, M., Yao, T., Jouzel, J., 2001. Tibetan Plateau summer monsoon northward extent revealed by measurements of water stable isotopes. J. Geophys. Res. Atmos. 106, 28081–28088.
Tian, L., Yao, T., Schuster, P.F., White, J.W.C., Ichiyanagi, K., Pendall, E., Pu, J., Wu, Y., 2003. Oxygen-18 concentrations in recent precipitation and ice cores on the Tibetan Plateau. J. Geophys. Res. Atmos. 108.
Tian, L., Yao, T., Li, Z., MacClune, K., Wu, G., Xu, B., Li, Y., Lu, A., Shen, Y., 2006. Recent rapid warming trend revealed from the isotopic record in Muztagata ice core, eastern Pamirs. J. Geophys. Res. Atmos. 111.
Vandenberghe, J., Renssen, H., van Huissteden, K., Nugteren, G., Konert, M., Lu, H., Dodonov, A., Buylaert, J.-P., 2006. Penetration of Atlantic westerly winds into central and east Asia. Quat. Sci. Rev. 25, 2380–2389.
Wang, R.L., Scarpitta, S.C., Zhang, S.C., Zheng, M.P., 2002. Later Pleistocene/Holocene climate conditions of Qinghai-Xizhang Plateau (Tibet) based on carbon and oxygen stable isotopes of Zabuye Lake sediments. Earth Planet. Sci. Lett. 203, 461–477.
Wang, S., Wang, E., Fang, X., Fu, B., 2008. Late Cenozoic systematic left-lateral stream deflections along the Ganzi-Yushu fault, Xianshuihe fault system, Eastern Tibet. Int. Geol. Rev. 50, 624–635.
Wang, Y., Liu, X., Herzschuh, U., 2010. Asynchronous evolution of the indian and east Asian summer monsoon indicated by Holocene moisture patterns in monsoonal central Asia. Earth Sci. Rev. 103, 135–153.
Wang, Y., Herzschuh, U., Shumilovskikh, L.S., Mischke, S., Birks, H.J.B., Wischnewski, J., Bohner, J., Schlutz, F., Lehmkuhl, F., Diekmann, B., Wünnemann, B., Zhang, C., 2014. Quantitative reconstruction of precipitation changes on the NE Tibetan Plateau since the Last Glacial Maximum - extending the concept of pollen source area to pollen-based climate reconstructions from large lakes. Clim. Past 10, 21–39.
Wang, Y.J., Cheng, H., Edwards, R.L., He, Y.Q., Kong, X.G., An, Z.S., Wu, J.Y., Kelly, M.J., Dykoski, C.A., Li, X.D., 2005. The Holocene Asian monsoon: links to solar changes and North Atlantic climate. Science 308, 854–857.
Wischnewski, J., Mischke, S., Wang, Y., Herzschuh, U., 2011. Reconstructing climate variability on the northeastern Tibetan Plateau since the last Lateglacial - a multi-proxy, dual-site approach comparing terrestrial and aquatic signals. Quat. Sci. Rev. 30, 82–97.
Witt, R., Günther, F., Lauterbach, S., Kasper, T., Mäusbacher, R., Yao, T., Gleixner, G., 2016. Biogeochemical evidence for freshwater periods during the Last Glacial Maximum recorded in lake sediments from Nam Co, south-central Tibetan Plateau. J. Paleolimnol. 55, 67–82.
Wu, T.W., Qian, Z.A., 2003. The relation between the Tibetan winter snow and the Asian summer monsoon and rainfall: an observational investigation. J. Clim. 16, 2038–2051.
Yao, T.D., Thompson, L.G., 1992. Trends and features of climatic changes in the past 5000 years recorded by the Dunde ice core. Annals of Glaciology. In: Hooke, R.L. (Ed.), 1992: Proceedings of the Symposium on Mountain Glaciology Relating to Human Activity, vol. 16, pp. 21–24.
Yao, T.D., Jiao, K.Q., Tian, L.D., Yang, Z.H., Shi, W.L., Thompson, L.G., 1996. Climatic variations since the little ice age recorded in the Guliya ice core. Sci. China Ser. B Earth Sci. 39, 587–596.
Yao, T., Masson-Delmotte, V., Gao, J., Yu, W., Yang, X., Risi, C., Sturm, C., Werner, M., Zhao, H., He, Y., Ren, W., Tian, L., Shi, C., Hou, S., 2013. A review of climatic controls on $\delta^{18}O$ in precipitation over the tibetan plateau: observations and simulations. Rev. Geophys. 51, 525–548.
Zhang, C., Mischke, S., 2009. A Lateglacial and Holocene lake record from the Nianbaoyeze Mountains and inferences of lake, glacier and climate evolution on the eastern Tibetan Plateau. Quat. Sci. Rev. 28, 1970–1983.
Zhao, Y., Yu, Z., Chen, F., Ito, E., Zhao, C., 2007. Holocene vegetation and climate history at Hurleg lake in the Qaidam Basin, northwest China. Rev. Palaeobot. Palynol. 145, 275–288.
Zhou, W.J., Dodson, J., Head, M.J., Li, B.S., Hou, Y.J., Lu, X.F., Donahue, D.J., Jull, A.J.T., 2002. Environmental variability within the Chinese desert-loess transition zone over the last 20, 000 years. Holocene 12, 107–112.